Available online at www.sciencedirect.com
ScienceDirect
Polymer 48 (2007) 116–128
polymer
www.elsevier.com/locate/polymer

Synthesis and light emitting properties of sulfide-containing polyfluorenes and their nanocomposites with CdSe nanocrystals: A simple process to suppress keto-defect

Chung-He Yang, Chetan Jagdish Bhongale, Cheng-Hsuan Chou, Sheng-Hsiung Yang, Chih-Nan Lo, Teng-Ming Chen, Chain-Shu Hsu*

Department of Applied Chemistry, National Chiao Tung University, 1001 Ta-Hsueh Road, Hsinchu 30010, Taiwan, ROC

Received 12 September 2006; received in revised form 6 November 2006; accepted 8 November 2006
Available online 28 November 2006

Abstract

A new series of sulfide-containing polyfluorene homopolymers and copolymers (**PFS**, **PF1**, **PF3** and **PF4**) comprising 9,9-di[11-(decylsulfanyl)undecyl] fluorene, 9,9-dihexylfluorene, triphenylamine or benzothiadiazole moieties were synthesized by Ni(0)-mediated Yamamoto-coupling and palladium-catalyzed Suzuki polymerizations. Three other polyfluorenes (**PF2**, **PF5** and **PFC6**) without sulfur atom in the alkyl side chains were also synthesized by a similar method for comparison purpose. These fluorene-based polymers were characterized using FT-IR spectroscopy, elemental analysis, DSC, TGA, photoluminescence (PL) and electroluminescence (EL) spectroscopies. The synthesized polymers **PFS** and **PF1**–**PF3** emit blue light at around 440–468 nm, while copolymers **PF4** and **PF5** emit green light at around 540 nm. In annealing experiments, these polymer films show better stability against thermal oxidation than polymer **PFC6**. Sulfide-containing polymers show not only good electroluminescent color stability, but their EL spectra also remain unchanged at high driving voltage. A multi-layer electroluminescent device with the configuration of ITO/PEDOT/**PF1**/CsF/Al exhibited a stable sky-blue emission with color coordinates (0.21, 0.23) at 10 V, which showed a maximum brightness of 2991 cd/m^2 at 8 V (75 mA/cm^2) and a maximum efficiency of 1.36 cd/A. Finally, by ligand exchange process, the sulfur element could form coordination bonding with quantum dots, and PLED devices using these new QDs-containing organic/inorganic hybrid materials as light-emitting layers exhibit superior or comparable EL performance compared to those without quantum dots.

Keywords: Polyfluorene; Keto-defect; Light-emitting diodes

1. Introduction

Since the first report of an electroluminescence device based on conjugated polymers by Burroughes et al. [1], this field has been extensively studied. Compared to inorganic or small organic molecules, organic conjugated polymers offer many advantages such as simple processing, high flexibility, potentially low power consumption, and uniformly covering large areas by spin coating in flat panel displays. By properly adjusting the chemical structure, one can fine-tune their optical and electrical properties, and get pure red, green, and blue light-emitting chromophores with narrow emitting spectra.

Polymers based on poly(phenylene vinylene) and poly(dialkylfluorene) show great promise and have evolved as most well-studied conjugated systems for organic light-emitting diode (OLED) application. Polyfluorenes, with their high photoluminescence (PL) quantum efficiencies, good thermal and chemical stabilities, excellent solubility in common organic solvents, can be used as a good blue-light emitter. By structural modification at the 9-position of the fluorene ring, one can easily synthesize different polyfluorene derivatives which

* Corresponding author. Tel./fax: +886 3 5131523.
E-mail address: cshsu@mail.nctu.edu.tw (C.-S. Hsu).

0032-3861/$ - see front matter © 2006 Elsevier Ltd. All rights reserved.
doi:10.1016/j.polymer.2006.11.012

possess good thermal stability and electroluminescent properties. However, polyfluorene tends to aggregate in the condensed phase and degrade the device performance with *n*-alkyl side chains resulting in a red-shifted fluorescence and lower PL intensity by exciton relaxation through lowering excimer trap process [2–8]. Spectral instability changes the emission light of polyfluorene from blue to greenish-blue region, and usually results in a broad band emission centered at around 530–540 nm with heat treatment, UV irradiation or applied electrical field. This is imputing to polyfluorene backbone degradation and named 'keto-defect' [3,7,9–11]. Continuing efforts have been made to reduce this phenomenon, which involve (1) synthesis of polymers that are thermally more stable [3a,d,12], (2) usage of bulky groups as end cappers to suppress excimer emission [3b,c,5], (3) insertion of the rigid bulky groups to C-9 position to prevent formation of excimers [4a,b,13,14], (4) copolymerization with sterically hindered groups, combining with spiro- or cross-linked hole-transporting materials to prevent aggregation [3c,5,15–18] and (5) bonding covalently with organic–inorganic hybrid materials (e.g. POSS) [19,20] to effectively improve electroluminescent characteristics.

Research on PLEDs has focused on the improvement of the emission efficiency of molecular semiconductors. Utilization of the nanocomposites to enhance the performance of PLEDs was proposed several years ago. Several studies have been carried out to enhance the current density, radiances, and power efficiency properties by mixing oxide nanoparticles (TiO_2, SiO_2) into electroluminescent polymer materials like MEH–PPV [21]. Moreover, photovoltaic efficiency of PPV derivatives could be improved by the incorporation of C_{60} nanoparticles [22]. Kim et al. reported the method of blending 5 nm gold nanoparticles in very low amounts into polyfluorene or PPV, resulting in an enhancement in quantum efficiency and oxidation stability [23]. Recently, Chou et al. reported that with the incorporation of surface-modified cadmium sulfide nanoparticles into dendron-substituted polyfluorene, the luminescence could be enhanced by as much as three times [24].

In earlier work, we have already reported the synthesis of sulfide-containing poly(1,4-phenylene vinylene) derivatives, and these polymers have the advantage of permitting the coordinate bonding of sulfur atoms with inorganic crystals (CdSe, ZnS) through ligand exchange process [25]. By incorporating **CdSe/ZnS** quantum dots onto sulfide-containing conjugated polymer S–PPV, the device performance was significantly improved as compared to the pristine polymers. Herein, we demonstrate the synthesis and characterization of series of fluorene-based copolymers with pendent sulfide groups attached on the C-9 positions of the fluorene unit. The thermal, electrochemical, optical, and other relevant physical properties of the synthesized polymers were also systematically studied. In addition, a series of PLED devices were also fabricated to study the electroluminescent (EL) properties of these polymers. Grafting a low percentage of **CdSe/ZnS** nanocrystals with sulfide-containing polyfluorene as active layers in the light-emitting diodes improved the efficiency of double-layer PLED device.

2. Experimental section

2.1. Characterization methods

IR spectra were recorded on a Perkin–Elmer 16PC FT-IR spectrometer. The chemical structures were confirmed using ^1H and ^{13}C NMR spectra measured on a Varian VXR-300 spectrometer (300 MHz). Differential scanning calorimetry (DSC) thermograms were recorded on a Perkin–Elmer Pyris Diamond DSC unit using a heating rate of 20 °C/min and a cooling rate of 50 °C/min. TGA thermograms were obtained on a Perkin–Elmer Pyris 1 TGA instrument with a heating rate of 10 °C/min. UV–Vis spectra were measured with an HP 8453 diode array spectrophotometer. PL spectra were obtained on a Hitachi F-4500 luminescence spectrometer, and the PL external quantum efficiencies were measured using an integrating sphere. Cyclic voltammetry (CV) measurements of the polymers were done in acetonitrile (CH_3CN) with 0.1 M tetrabutylammonium hexafluorophosphate ($TBAPF_6$) as the supporting electrolyte at a scan rate of 50 mV/s. Platinum wires were used as both the counter and working electrodes, silver/silver ions (Ag in 0.1 M $AgNO_3$ solution, from Bioanalytical Systems, Inc.) were used as the reference electrode, and ferrocene as an internal standard.

2.2. Fabrication and characterization of PLEDs

Double-layer PLED devices were fabricated as sandwich structures between cathode (Ca) and indium-tin oxide (ITO) anodes. ITO-coated glass substrates were cleaned sequentially in ultrasonic baths of detergent, 2-propanol/deionized water (1:1 volume) mixture, toluene, deionized water, and acetone. A 50 nm thick hole injection layer of poly(3,4-ethylenedioxythiophene) doped with poly(styrenesulfonate) (PEDOT:PSS) was spin-coated on top of ITO from a 0.7 wt% dispersion in water and dried at 120 °C for 1 h under vacuum. Thin films of polymers from a 1.5 wt% toluene solution were spin-coated upon the PEDOT layer and dried at 70 °C under vacuum for 1 h. The film thickness obtained was ca. 45 nm, which was measured by an Alpha-Step 500 surface profiler (KLA Tencor, Mountain View, CA). The coating thickness of PEDOT and polymers together was about 1000 Å, and the active areas were 0.04 cm^2, defined by the area overlapped by the anode and the cathode. The TPBI layer was grown by thermal sublimation under vacuum (3×10^{-6} Torr) and was used as an electron transporting layer, which would also block holes and confine excitons. The CsF layer was also grown by thermal sublimation under vacuum (3×10^{-6} Torr) and used as an electron injection layer. Finally, 35 nm Ca and 100 nm Al electrodes were thermally evaporated through a shadow mask onto the polymer films using an AUTO 306 vacuum coater (BOC Edwards, Wilmington, MA); typical evaporations being carried out at base pressure lower than 2×10^{-6} Torr. The PLED characterization was carried out by a Keithley 2400 source-measure unit. The brightness was further measured using a Photo Research PR650 spectrophotometer.

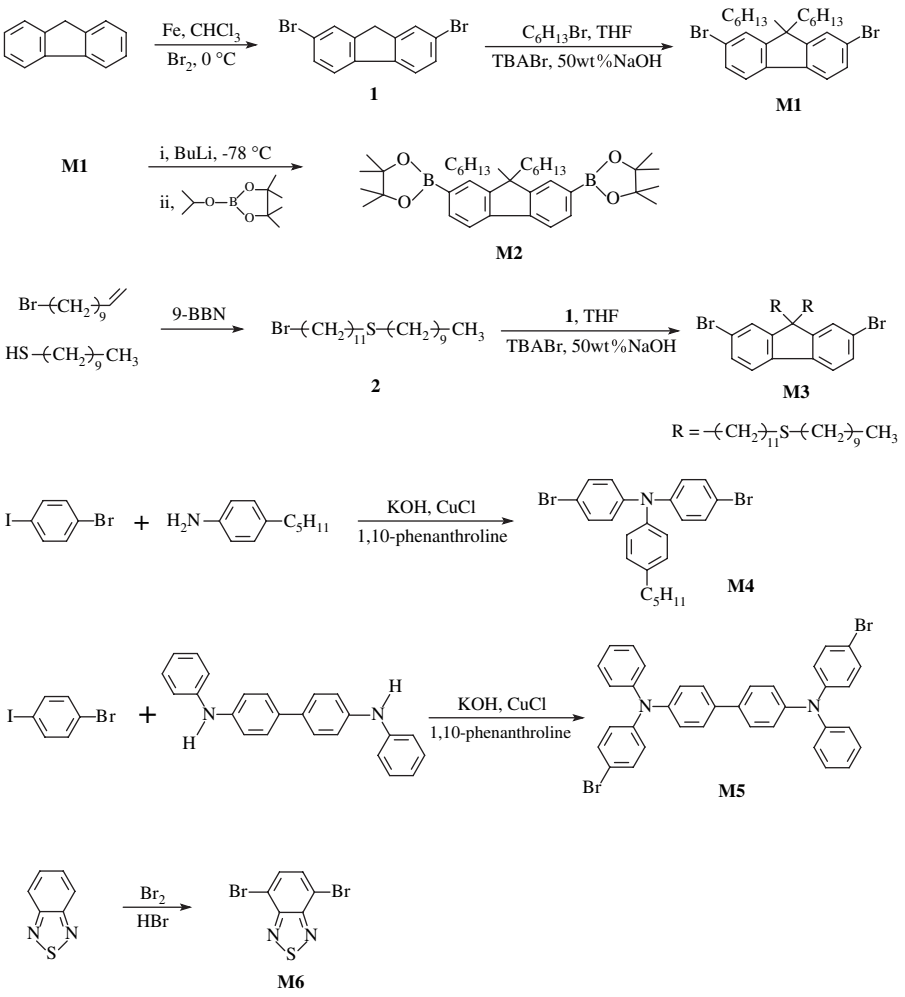

Scheme 1. Synthesis of monomers **M1**–**M6**.

2.3. Materials

Starting materials such as fluorene, *n*-butyllithium were purchased from TCI. The Suzuki-coupling catalyst, tetrakis(triphenylphosphine)palladium(0) and Yamamoto polymerization catalyst, bis(1,5-cyclooctadienyl)nickel(0), 2,2′-bipyridinyl, and 1,5-cyclooctadiene were purchased from Aldrich and handled under inert argon atmosphere. All other chemicals were used as received from commercial sources without further purification, except tetrahydrofuran (THF) and toluene which were distilled over sodium/benzophenone and calcium hydride, respectively. The synthesis of monomers **M1**–**M5** is shown in Scheme 1. 2,7-Dibromofluorene (**1**), 2,7-dibromo-9,9-dihexylfluorene (**M1**) [26], 11-bromoundecyl decyl sulfide (**2**) [27] and 4,7-dibromo-1,2,3-benzothiadiazole (**M6**) [28] were prepared following the published procedures. (**1**): white crystal, yield 91%, mp = 161–163 °C. **M1**: white crystal, yield 89%, mp = 64–65 °C. (**2**): white solid, yield 83%, mp = 25–26 °C. **M6**: yellow needle crystals, yield 98%, mp = 187–188 °C.

2.3.1. 2,7-Bis(4,4,5,5-tetramethyl-1,3,2-dioxaborolan-2-yl)-9,9-dihexylfluorene (*M2*)

M2 was prepared following the modified procedure from 2,7-dibromo-9,9-dihexylfluorene (**M1**). White solid, yield 81%, mp = 185–186 °C. ^{1}H NMR (300 MHz, $CDCl_3$, δ ppm): 7.78 and 7.71 (d, 4H, fluorene ring), 7.68 (s, 2H, fluorene ring), 1.98 (t, 4H, H-alkyl), 1.36 (s, 24H, CH_3), 1.11–0.98 (m, 16H, CH_2), 0.72 (t, 6H, CH_3). ^{13}C NMR (75 MHz, $CDCl_3$, δ ppm): 150.44, 143.30, 133.62, 129.29, 119.34 (fluorene ring), 83.61 (C-alkyl), 55.15 (C_9, fluorene ring), 40.49, 31.48, 29.58, 24.31, 23.54, 22.53, 13.48 (C-alkyl). MS (EI-MS) *m*/*z*: 586.4. Elemental Anal. Calcd. for $C_{37}H_{60}B_2O_4$: C, 75.7; H, 9.62. Found: C, 75.62; H, 9.73.

2.3.2. 2,7-Dibromo-9,9-di[11-(decylsulfanyl)undecyl]-fluorene (*M3*)

To a solution of *t*-BuOK (5.2 g, 46.3 mmol) and 11-bromoundecyl decyl sulfide (**2**) (8.67 g, 21.3 mmol) in a 100-mL three-neck flask, a solution of 2,7-dibromofluorene (3 g, 9.26 mmol) in 15 mL THF was added drop wise under nitrogen atmosphere. The reaction mixture was refluxed for 12 h at 80 °C. After cooling to room temperature, the solution was extracted with hexane, the collected organic phase was dried over magnesium sulfate and filtered, rotary evaporated to remove solvent. The crude product was isolated, and further purified by column chromatography over silica gel by eluting with ethyl acetate/hexane = 1:10 to yield 3.81 g (88%) of white crystals, mp = 41–42 °C.

^{1}H NMR (300 MHz, $CDCl_3$, δ ppm): 7.50–7.41 (m, 6H, fluorene ring), 2.49–2.42 (t, 8H, CH_2S), 1.90–1.85 (t, 4H, H-alkyl), 1.56–1.17 (m, 68H, CH_2), 0.87 (s, 12H, CH_3). ^{13}C NMR (75 MHz, $CDCl_3$, δ ppm): 152.49, 139.02, 130.11, 126.14, 121.43, 121.08 (fluorene ring), 55.64 (C_9, fluorene ring), 40.09, 32.15, 31.86, 29.79, 29.70, 29.53, 29.50, 29.42, 29.29, 29.23, 29.19, 29.12, 28.92, 28.90, 23.57, 22.65, 14.08 (C-alkyl). MS (FAB-MS) *m/z*: 977.2. Elemental Anal. Calcd. for $C_{55}H_{92}Br_2S_2$: C, 67.6; H, 9.49. Found: C, 67.72; H, 9.53.

2.3.3. *N,N-Di(4-bromophenyl)-N-(4-pentylphenyl)amine (**M4**)*

A mixture of 1-bromo-4-iodobenzene (13.32 g, 47 mmol), 4-pentylaniline (3.5 g, 21.4 mmol), 1,10-phenanthroline (0.385 g, 2.14 mmol), CuCl (0.212 g, 2.14 mmol) and KOH (12 g, 214 mmol) in 120 mL toluene was refluxed at 120 °C for 12 h. The solution was cooled to room temperature and then the solvent was removed by evaporation. The collected organic layer was mixed with 50 mL of ethyl acetate and extracted with 50 mL of water. The organic layer was dried over anhydrous magnesium sulfate. After the solvent was removed by rotary evaporator, the crude product was isolated by filtration, and further purified by column chromatography using silica gel by eluting with ethyl acetate/hexane = 1:5 to yield 7.3 g (72%) of white crystals, mp = 57–58 °C. ^{1}H NMR (300 MHz, $CDCl_3$, δ ppm): 6.86–7.32 (m, 12H, aromatic protons), 2.54 (t, 2H, $-CH_2-(CH_2)_3-CH_3$), 1.23–1.59 (m, 6H, $-CH_2-(CH_2)_3-CH_3$), 0.88 (t, 3H, $-CH_3$). ^{13}C NMR (75 MHz, $CDCl_3$, δ ppm): 147.52, 144.40, 139.72, 132.59, 128.23, 124.21, 121.37, 114.28 (aromatic ring), 36.92, 31.66, 31.02, 22.43, 14.29, (C-alkyl). MS (EI-MS) *m/z*: 473.2. Elemental Anal. Calcd. for $C_{23}H_{23}Br_2N$: C, 58.37; H, 4.9; N, 2.96. Found: C, 58.67; H, 5.06; N, 2.90.

2.3.4. *4,4′-Bis[(N-p-bromophenyl)-N-phenylamino]biphenyl (**M5**)*

The procedures for the synthesis of **M5** were similar to that of **M4**, using 1-bromo-4-iodobenzene (9.25 g, 32.69 mmol), *N,N′*-diphenyl benzidine (5 g, 14.86 mmol), 1,10-phenanthroline (0.14 g, 0.74 mmol), CuCl (0.08 g, 0.74 mmol) and KOH (6.67 g, 118.88 mmol) as starting materials. Monomer **M5** was purified by column chromatography on silica gel by eluting with ethyl acetate/dichloroethane = 1:6 to yield 3.81 g (40%) white crystals, mp = 171–172 °C. ^{1}H NMR (300 MHz, $CDCl_3$, δ ppm): 7.43 (d, 4H, aromatic protons), 7.34–7.24 (m, 9H, aromatic protons), 7.11–7.04 (m, 9H, aromatic protons), 6.97 (d, 4H, aromatic protons). ^{13}C NMR (75 MHz, $CDCl_3$, δ ppm): 147.16, 146.80, 146.32, 135.09, 132.18, 129.48, 127.45, 125.28, 124.52, 124.28, 123.38, 114.35 (aromatic ring). MS (EI-MS) *m/z*: 648.0. Elemental Anal. Calcd. for $C_{36}H_{26}Br_2N_2$: C, 66.89; H, 4.05; N, 4.33. Found: C, 66.21; H, 3.89; N, 4.02.

2.4. Polymerization

2.4.1. *The synthetic procedures for homopolymers **PFS** and **PFC6***

Homopolymers (**PFS** and **PFC6**) were synthesized by nickel(0)-catalyzed polymerizations [29] (Scheme 2). A typical synthetic procedure of **PFS** is given as follows. A mixture of bis(1,5-cyclooctadiene)nickel(0) (560 mg, 2.05 mmol), 2,2′-bipyridinyl (320 mg, 2.05 mmol), and 1,5-cyclooctadiene (220 mg, 2.05 mmol) was added to a 50 mL flask containing 10 mL of DMF and 10 mL of toluene. The solution was preheated at 60 °C under nitrogen atmosphere for 30 min, and then 5 mL of anhydrous toluene was added to the mixture. **M2** (500 mg, 1.02 mmol) was added to the flask and polymerization temperature was maintained at 80 °C for 72 h. *N,N*-Bis(4-methylphenyl)-*N*-(4-bromophenyl)amine was added as an end-capping reagent [30]. After polymerization was completed, each polymer was precipitated from a mixture of concentrated HCl, methanol, and acetone with equal volume. The isolated polymers were dissolved in toluene and further reprecipitated in methanol and dried under vacuum. Dialysis of the obtained polymers was done by immersing the polymer in acetone solution to remove oligomers. The yields of these two homopolymers were 73% and 85%, respectively.

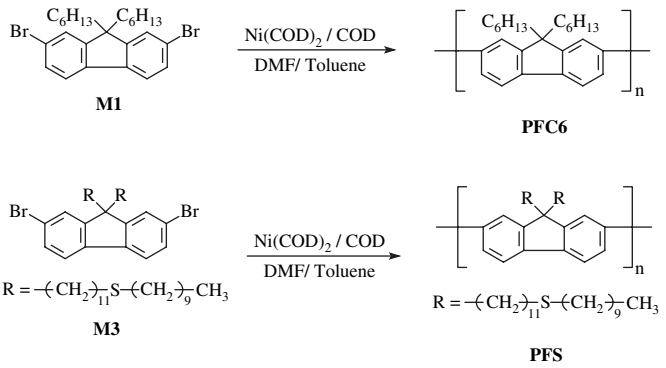

Scheme 2. Synthesis of polymers **PFC6** and **PFS**.

2.4.2. *The synthetic procedures for copolymers **PF1–PF5***

The copolymers of **PF1–PF5** were prepared via palladium-catalyzed Suzuki-coupling reaction [31] of the diboronic ester monomer **M2** with dibromo monomers **M1**, **M3–M6** (Scheme 3). The monomer feed ratios used in the polymerization are also given in Scheme 3. A typical synthetic procedure of **PF1** is given as follows. A mixture of **M2** (0.40 g, 0.68 mmol), **M3** (0.33 g, 0.34 mmol), and **M4** (0.16 g, 0.34 mmol) was added to a 50 mL flask containing 10 mL of toluene. Polymerization was carried out using $Pd(PPh_3)_4$ as the catalyst in a mixture of toluene and aqueous K_2CO_3 (2.0 M) in the presence of aliquat 336 as a phase transfer reagent. The solution was first put under the protection of argon and refluxed with vigorous stirring at 85 °C in oil bath for 4 days. *N,N*-Bis(4-methylphenyl)-*N*-(4-bromophenyl)amine was added for end-capping the boronic ester for 6 h. *N,N*-Di-(4-methylphenyl)-*N*-[4-(4,4,5,5-tetramethyl-1,3,2-dioxaborolan-2-yl)phenyl]amine was then added into the mixture for end-capping the bromo active site for additional 6 h. After cooling, the reaction mixture was precipitated from methanol to get polymers. This was followed by immersing the solid material in acetone solution to remove oligomers and catalyst residues. The precipitate was collected by filtration, re-dissolved

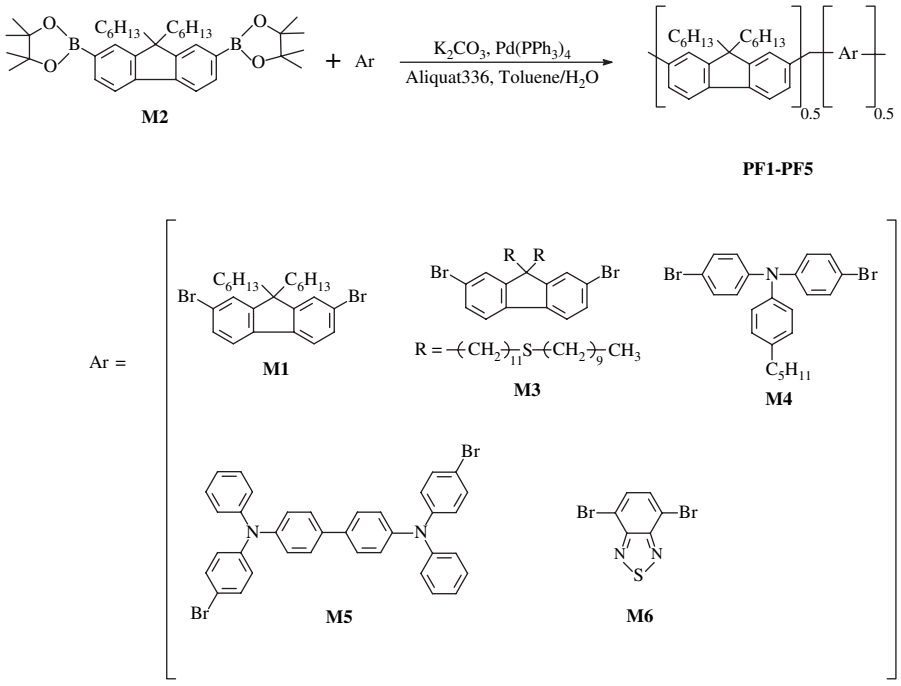

Monomers \ Polymers	PF1	PF2	PF3	PF4	PF5
M1 (mol%)		25			25
M2 (mol%)	50	50	50	50	50
M3 (mol%)	25		37.5	25	
M4 (mol%)	25	25		10	10
M5 (mol%)			12.5		
M6 (mol%)				15	15

Scheme 3. Synthesis of polymers **PF1**–**PF5** and the composition of the studied polymers.

in THF, and then reprecipitated in methanol, and finally dried under vacuum oven. The yields of these five copolymers were in the range of 62–90%.

*2.4.3. Homopolymer **PFS***

Yield of **PFS**: 73%. ^{1}H NMR (300 MHz, $CDCl_3$, δ ppm): 7.53–7.39 (m, aromatic protons), 2.50–2.41 (t, CH_2S), 1.90–0.88 (m, alkyl protons). Elemental Anal. Calcd. for $C_{55}H_{92}S_2$: C, 80.88; H, 11.27. Found: C, 79.12; H, 10.35.

*2.4.4. Homopolymer **PFC6***

Yield of **PFC6**: 85%. ^{1}H NMR (300 MHz, $CDCl_3$, δ ppm): 7.64–7.38 (m, aromatic protons), 1.88–0.76 (m, alkyl protons). Elemental Anal. Calcd. for $C_{25}H_{32}$: C, 90.36; H, 9.64. Found: C, 88.82; H, 10.42.

*2.4.5. Copolymer **PF1***

Yield of **PF1**: 82%. ^{1}H NMR (300 MHz, $CDCl_3$, δ ppm): 7.62–6.85 (m, aromatic protons), 2.84–2.30 (m, $-CH_2-$), 1.48–0.83 (m, alkyl protons). Elemental Anal. Calcd. for $C_{128}H_{179}NS_2$: C, 85.6; H, 10.05; N, 0.78. Found: C, 83.87; H, 9.70; N, 0.80.

*2.4.6. Copolymer **PF2***

Yield of **PF2**: 78%. ^{1}H NMR (300 MHz, $CDCl_3$, δ ppm): 7.68–6.82 (m, aromatic protons), 2.82–2.25 (m, $-CH_2-$), 1.49–0.81 (m, alkyl protons). Elemental Anal. Calcd. for $C_{98}H_{119}N$: C, 89.78; H, 9.15; N, 1.07. Found: C, 88.1; H, 8.21; N, 1.21.

*2.4.7. Copolymer **PF3***

Yield of **PF3**: 67%. ^{1}H NMR (300 MHz, $CDCl_3$, δ ppm): 8.10–6.85 (m, aromatic protons), 2.85–2.28 (m, $-CH_2-$), 1.46–0.83 (m, alkyl protons). Elemental Anal. Calcd. for $C_{150.5}H_{215}NS_3$: C, 84.68; H, 10.15; N, 0.656. Found: C, 85.23; H, 9.05; N, 0.82.

*2.4.8. Copolymer **PF4***

Yield of **PF4**: 90%. ^{1}H NMR (300 MHz, $CDCl_3$, δ ppm): 8.12–6.96 (m, aromatic protons), 2.86–2.32 (m, $-CH_2-$), 1.42–0.84 (m, alkyl protons). Elemental Anal. Calcd. for $C_{294.5}H_{416}N_4S_5$: C, 84.77; H, 10.05; N, 1.34. Found: C, 82.74; H, 9.55; N, 1.26.

*2.4.9. Copolymer **PF5***

Yield of **PF5**: 88%. ^{1}H NMR (300 MHz, $CDCl_3$, δ ppm): 8.05–6.83 (m, aromatic protons), 2.84–2.28 (m, $-CH_2-$), 1.46–0.83 (m, alkyl protons). Elemental Anal. Calcd. for $C_{439}H_{536}N_{12}S_3$: C, 89.05; H, 9.06; N, 1.89. Found: C, 88.0; H, 8.54; N, 1.68.

2.5. Synthesis of *PF1* and *CdSe/ZnS* nanocomposites

CdSe/ZnS nanocrystals were prepared following the published procedures [25], and the size of the nanocrystals was about 7.0 nm as determined by TEM. Generally, the procedure for ligand exchange reaction was described as follows. A solution of the sulfide-containing ligand **PF1** (20 mg in 1 mL of toluene) was added to the colloidal solution of CdSe nanocrystals (10 mg in 1 mL of toluene). The mixture was then stirred at constant temperature. The reaction status was confirmed by FT-IR. After ligand exchange process [25,37], the solution was poured into methanol to give the final polymer. The yields of obtained nanocomposites were in the range of 75–90%. TEM images of the nanocomposites also showed that CdSe nanocrystals were mono-dispersed with a diameter of about 7 nm. It indicates that QDs exactly exist inside the polymers.

3. Results and discussion

3.1. Synthesis and characterization

The synthesis of monomers **M1**–**M5** is shown in Scheme 1. Monomer **M3** was synthesized by reaction between 2,7-dibromofluorene and 11-bromoundecyl decyl sulfide in the presence of excess base. The sulfur atom in **M3** can serve as the ligand for **CdSe/ZnS** quantum dots which can be attached via simple ligand exchange procedure. The properties of these QD-related nanocomposites will be discussed later. Homopolymers **PFS** and **PFC6** were synthesized via Yamamoto-coupling method; this is to compare the thermal and electroluminescent properties with different alkyl chains. However, the EL performance of fluorene-based homopolymer is usually not high because of the charge imbalance, and the homopolymer only emits light in the blue region. For these reasons, we synthesized some other copolymers **PF1**–**PF5** via Suzuki-coupling, with triphenylamine (TPA) containing monomers and BTDZ to balance the charge ability and tune emissive colors of these polyfluorenes. TPA compounds are well-known hole-transporting materials. Two TPA-containing monomers (**M4** and **M5**) were synthesized by the Wittig–Horner reaction between *N*-(4-bromophenyl)-*N*-(4-formylphenyl) aniline and 4,4′-bis(diethylphosphinatylmethyl)biphenyl. These two TPA derivatives could fine-tune the EL emission wavelength of polyfluorenes in the range 450–470 nm and substantially improve the EL performance. Monomer **M6** (BTDZ) is used as comonomer in the polyfluorene backbone. Yellow-green light is emitted via energy transfer from fluorene to BTDZ. The chemical structures of the resulting polymers utilizing Yamamoto and Suzuki-coupling methods were further confirmed by ^{1}H NMR and elemental analyses. The actual ratio calculated from elemental analyses of C, H and N was in good agreement with the feeding ratios of the monomers, as stated above. Slight deviations might be caused by two end-capping reagents (*N*,*N*-bis(4-methylphenyl)-*N*-(4-bromophenyl)amine and *N*,*N*-di(4-methylphenyl)-*N*-[4-(4,4,5,5-tetramethyl-1,3,2-dioxaborolan-2-yl)-phenyl]amine). The obtained copolymers are completely soluble in common organic solvents, such as toluene, THF, and chloroform. The $\overline{M}_n$ and the $\overline{M}_w$ of these polymers determined by GPC were in the range from 1.03×10^4 to 3.09×10^4 and from 2.02×10^4 to 3.43×10^4 g/mol, respectively, with the polydispersity index less than 3.01 (see Table 1).

Table 1
Average molecular weights and thermal properties of polymers **PFS**, **PF1**–**PF5** and **PFC6**

Polymer	$\overline{M}_n$[a] ($\times 10^{-3}$)	$\overline{M}_w$[a] ($\times 10^{-3}$)	PDI ($\overline{M}_w/\overline{M}_n$)	T_d[b] (°C)	T_g[c] (°C)
PFS	23.7	34.3	1.45	353.3	58.3
PF1	30.9	34.3	1.11	373.7	83.6
PF2	20.4	29.6	1.45	372.0	81.6
PF3	13.9	20.2	1.45	369.1	87.3
PF4	10.3	31.0	3.01	349.0	82.0
PF5	17	26	1.59	351.8	83.0
PFC6	18.5	24.3	1.31	344.1	54.0

[a] Determined by GPC by eluting with THF, by comparison with polystyrene standards.
[b] Temperature at which a 5% weight loss occurred was determined at a heating rate of 10 °C/min under a nitrogen atmosphere.
[c] The value of T_g was determined at a heating rate of 20 °C/min under a nitrogen atmosphere.

3.2. Thermal properties

Good thermal stability is very important for the application of conjugated polymers in flat panel displays. The thermal stability of these polymers was evaluated by DSC and TGA under nitrogen atmosphere. Table 1 lists the thermal decomposition temperatures (T_d, 5% weight loss) and the glass transition temperatures (T_g) of these six polymers. Polymers **PF1**–**PF5** show glass transition temperature at around 80 °C, which is much higher than that of poly(9,9-dioctylfluorene) ($T_g = 51$ °C) [32]. As revealed by TGA, these polymers also exhibit good thermal stability with 5% weight loss occurring at 350 °C.

3.3. Photoluminescence properties

The fluorescent wavelength of a polymer film fundamentally depends on the band gap between the HOMO and LUMO, which depends on delocalization of π-electrons along the polymer backbone. The characteristic peak in the emission spectrum arises as an excited electron relaxes into vibronic energy level of the HOMO. The optical spectra of conjugated polymers are typically broad, which is due to the coupling of several different vibronic modes. Fig. 1 reveals the normalized absorption and photoluminescence spectra of polymers in dilute toluene solutions. The absorptions located in the range

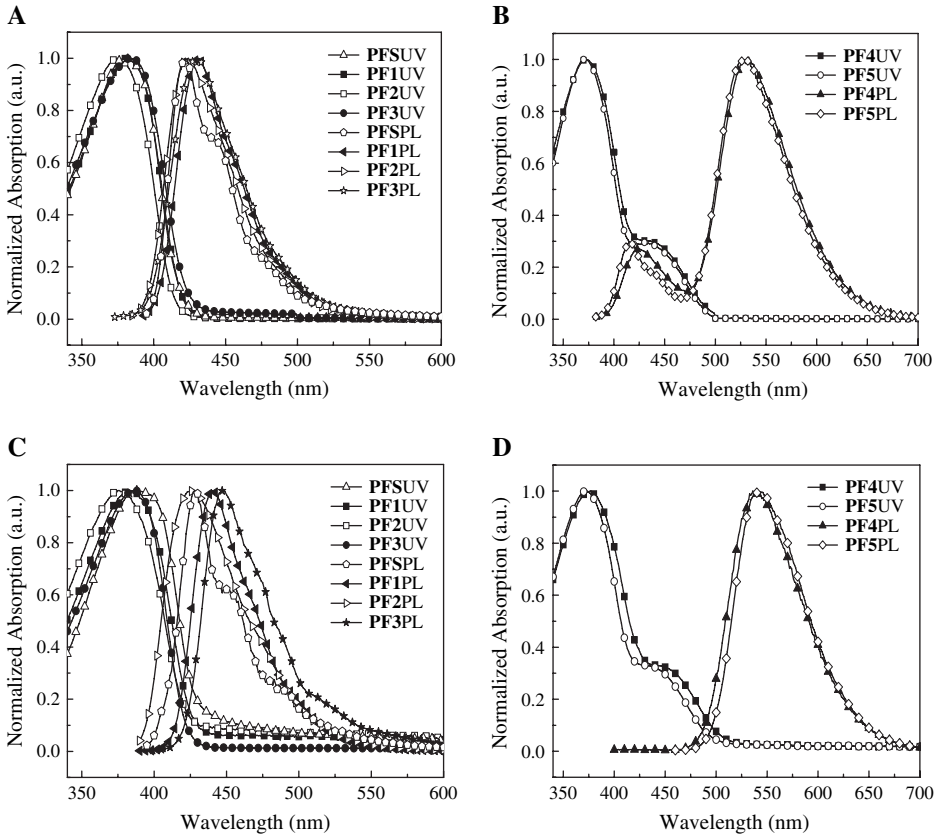

Fig. 1. Normalized UV–vis absorption and PL spectra of polymers (A) **PFS**, **PF1**, **PF2**, **PF3** in 10^{-5} M toluene solution, (B) **PF4**, **PF5** in 10^{-5} M toluene solution, (C) **PFS**, **PF1**, **PF2**, **PF3** in pristine films, and (D) **PF4**, **PF5** in pristine films.

from 372 to 386 nm were due to π–π* transition of conjugated polyfluorene backbone. The blue emission of polyfluorene around 430 nm could be effectively quenched by introducing BTDZ group into the main chain of polyfluorene copolymer and dominated by a green light peaked at 540 nm for **PF4** (see Fig. 1(B)). It also reveals the effective energy transfer from photo-generated excitons on the polyfluorene segment to BTDZ groups. The wavelengths of UV–vis absorption and PL emission maxima of these polymers in dilute toluene solution (10^{-5} M) and in solid state are summarized in Table 2. For comparison purpose, we synthesized **PF2** and **PF5** which have very similar chemical structures with **PF1** and **PF4**, except that both **PF2** and **PF5** contain alkyl side groups without sulfur atoms. It is no surprise that both polymers show no difference in their UV absorption and PL emission spectra because of the similar polymer backbone. In comparison with dilute solutions, the emission spectra of polymers in film state are slightly red-shifted and can be attributed due to the aggregation of polymer chains. Table 2 also outlines PL quantum efficiencies of polymers in both solution and film states as measured by the integrating sphere. These polymers exhibit very high PL efficiencies from 56% to 82% in toluene solution.

Table 2
Optical properties of polymers **PFS**, **PF1–PF5**

Polymer	UV absorption (λ_{max} (nm))		PL (λ_{max} (nm))		PL_{eff} (%)	
	Toluene	Film	Toluene	Film	Toluene	Film
PFS	381	387	422	428	56.2	23.1
PF1	383	383	431	440	82.5	54.3
PF2	384	386	430	448	69.2	42.8
PF3	375	376	424	427	75.6	46.7
PF4	373	377	425, 532	536	73.8	33.3
PF5	372	377	418, 527	541	70.7	35.2

3.4. Annealing experiment

According to the previous literature [33], when the temperature inside PLED devices exceeds 86 °C, the optical properties, especially luminescence and color stability of light-emitting material are strongly affected. The origin of the green emission in polyfluorene-based conjugated polymers has been mostly attributed to aggregation and/or excimer formation or keto defects caused due to formation of fluorenone units in the PF backbone [3,7,9–11]. The utility of polyfluorenes is limited because of their tendency to undergo interchain aggregation. Furthermore, when the solid films of the polymers are maintained under the higher temperature above T_g, the keto-defect would appear and emit green light around 540 nm. In order to investigate the thermal stability and the keto defects of the prepared polymers, thin films were annealed in the oven at 200 °C for 20 h in air.

Fig. 2(A) and (B), shows the normalized photoluminescence (PL) spectra of homopolymers **PFC6** and **PFS** films at room temperature 25 °C and thermally annealed at 200 °C for

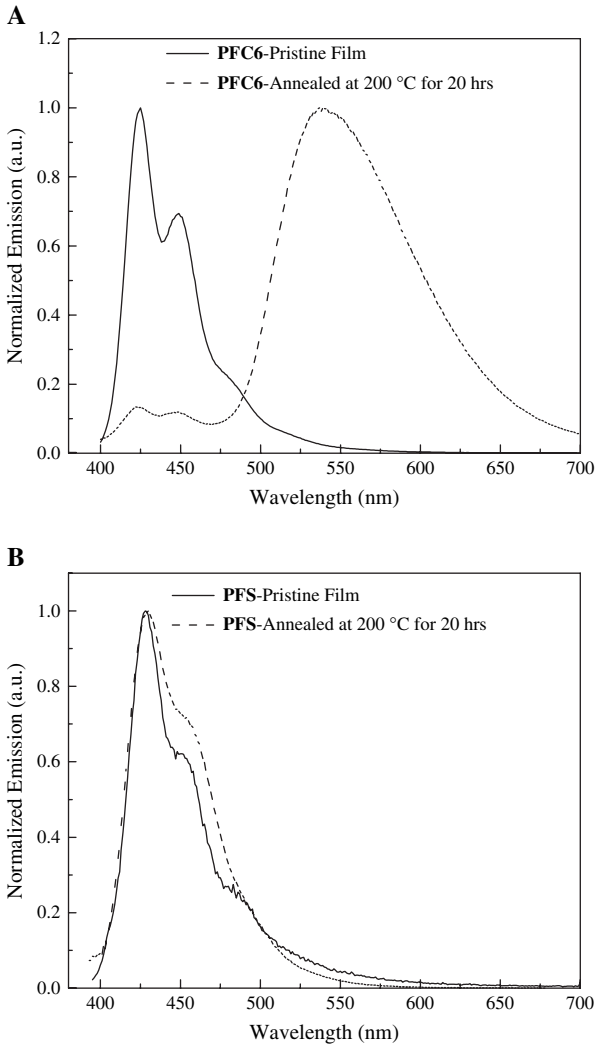

Fig. 2. Normalized PL spectra of (A) **PFC6** and (B) **PFS** in solid state before and after annealing at 200 °C for 20 h under air.

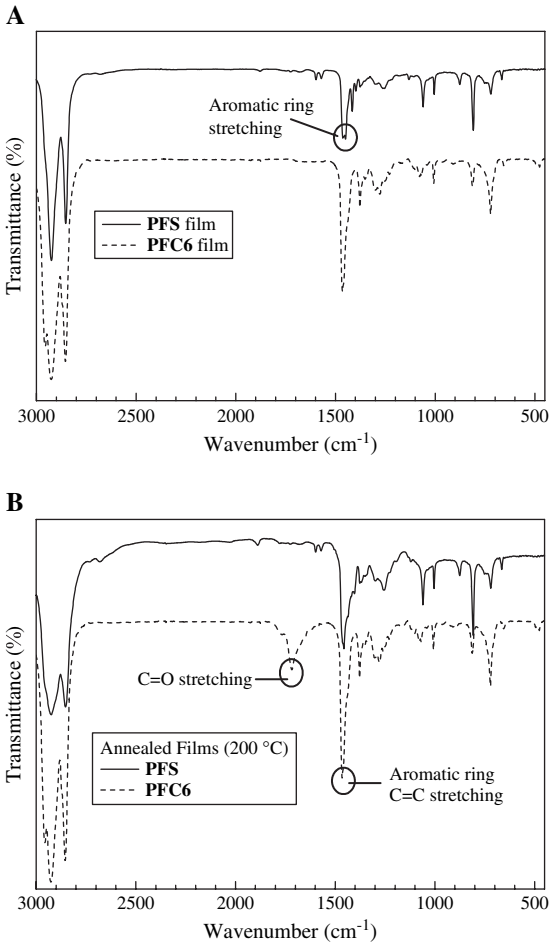

Fig. 3. FT-IR spectra of fluorene-based polymers **PFS** and **PFC6** (A) at 25 °C (B) after annealing at 200 °C for 20 h.

20 h. In Fig. 2(A), the **PFC6** film annealed at 200 °C for 1 h shows a strong green emission at a longer wavelength of about 537 nm, which is attributed to the excimer emission in comparison with the fresh films while the absorption λ_{max} remained at 425 nm. Compared to **PFC6**, the PL spectrum of **PFS** shows a small shoulder under similar heating conditions. The unchanged emission λ_{max} before and after heating suggests that the polymer did not change its conjugated structure during the thermal treatment. The 537 nm peak showed in Fig. 2(A) is due to the combination effect of keto-defect and polymer chain aggregation. The defect phenomena are generally appeared in alkyl-substituted polyfluorene. This unchanged PL curve of polymer **PFS** strongly hints that sulfide-containing polyfluorene may inhibit the aggregation of polymer chains under thermal annealing. Fig. 3 shows the FT-IR spectra of **PFC6** and **PFS** films after annealed at 200 °C for 20 h. No obvious fluorenone (C═O) characteristic IR peak at around 1720 cm^{-1} peak was found for **PFS**; however, for polymer **PFC6**, the keto peak at 1721 cm^{-1} appears. This result suggests that the existence of sulfur moiety could effectively suppress the keto formation and aggregation of polymer chains.

3.5. Electrochemical properties

The electrochemical behaviors of these polymers were investigated by cyclic voltammetry (CV). The corresponding highest-occupied molecular orbital (HOMO) and lowest-unoccupied molecular orbital (LUMO) energy levels were estimated from the onset of the redox potentials. HOMO and LUMO levels of the chromophores were calculated according to empirical formulae $E_{HOMO} = -(E_{ox} + 4.4)$ (eV) and $E_{LUMO} = -(E_{red} + 4.4)$ (eV) [34]. From the difference of the onset potentials and the optical band gaps (E_g) calculated from the onsets of UV absorption spectra, the energy levels, the oxidation and reduction potentials were determined and are summarized in Table 3. The reversible oxidation curve of **PFS** with onset around 1.29 V could be assigned to the p-doping oxidation potential of polyfluorene main chains. Meanwhile, the electrochemical oxidation of polymers **PF1–PF3** all exhibit similar two peaks at 0.81 and 1.08 V vs Ag/Ag^+, and these characteristic peaks are originated from triphenylamine and fluorene units, respectively [35]. However, the BTDZ

Table 3
Electrochemical properties of **PFS** and **PF1–PF5**

Sample	Optical band gap[a] (eV)	E_{ox}[b] (V)	E_{red}[b] (V)	HOMO[c] (eV)	LUMO[c] (eV)
PFS	2.91 (426)	1.29	−1.62	−5.69	−2.78
PF1	2.91 (426)	1.09	−1.82	−5.49	−2.58
PF2	2.93 (423)	1.08	−1.85	−5.48	−2.54
PF3	2.95 (420)	1.08	−1.87	−5.48	−2.53
PF4	2.42 (511)	1.26	−1.16	−5.66	−3.24
PF5	2.48 (500)	1.23	−1.25	−5.63	−3.15

[a] The optical band gap estimated from the onset wavelength (value in parentheses) of UV–vis spectra of the polymer film.
[b] The E_{ox} and the E_{red} are the onset potentials of oxidation and reduction, respectively.
[c] Calculated from the empirical formula, $E_{(HOMO)} = -(E_{ox} + 4.40)$ (eV), $E_{(LUMO)} = -(E_{red} + 4.40)$ (eV).

(**M6**) moiety in **PF4** and **PF5** is more electron-deficient and easier to be reduced as compared with another system (**PF1–PF3**) having **M3–M5** components. Since BTDZ has a smaller gap than polyfluorene, the excitation energy on the fluorene segments can transfer to the BTDZ unit with highly efficient green light.

3.6. Electroluminescence properties

To evaluate the electroluminescent properties of these sulfide-containing polyfluorenes, different types of light-emitting devices were fabricated and the device performances were examined. The energy diagram of these polymers and a general device architecture ITO/PEDOT:PSS/polymer (40 nm)/Ca (35 nm)/Al (100 nm) are shown in the Fig. 4(A) and (B), respectively. In the double-layer device A, poly(3,4-ethylenedioxythiophene) (PEDOT) was used as the hole-injecting layer. The device performances of **PF1–PF5** are shown in Table 4. After introducing the sulfide-containing long alkyl side chain into the polyfluorene, no noticeable difference in the maximum luminance and yield was observed (**PF1/PF2**, **PF4/PF5**). The relevant results showed a maximum brightness of 990 cd/m^2 (at 10 V) and a maximum yield of 0.15 cd/A (330 mA/cm^2) for **PF1**, while a maximum brightness of 700 cd/m^2 (at 11 V) and a maximum yield of 0.11 cd/A (636 mA/cm^2) for **PF3**, whereas **PF4** showed a maximum brightness of 1743 cd/m^2 (at 11 V) and a maximum yield of 0.60 cd/A (220 mA/cm^2). The EL spectra of **PF1** and **PF4** were also very similar to those of **PF2** and **PF5**, respectively. It also suggests that the incorporation of sulfur atom into the polymers does not influence the conjugation length of these polymers.

In order to improve the EL efficiencies of these sulfide-containing polyfluorene devices, we fabricated device B with the detailed structure ITO/PEDOT:PSS/polymer (40 nm)/CsF (2 nm)/Al (100 nm). A thin layer of CsF introduced between light-emitting polymer and Al electrode enhances electron injection and leads to a higher electroluminance [36]. With the CsF as the electron-donator, efficiency and luminance could be effectively enhanced, by improving the electron–hole recombination of the materials. Table 4 summarizes the

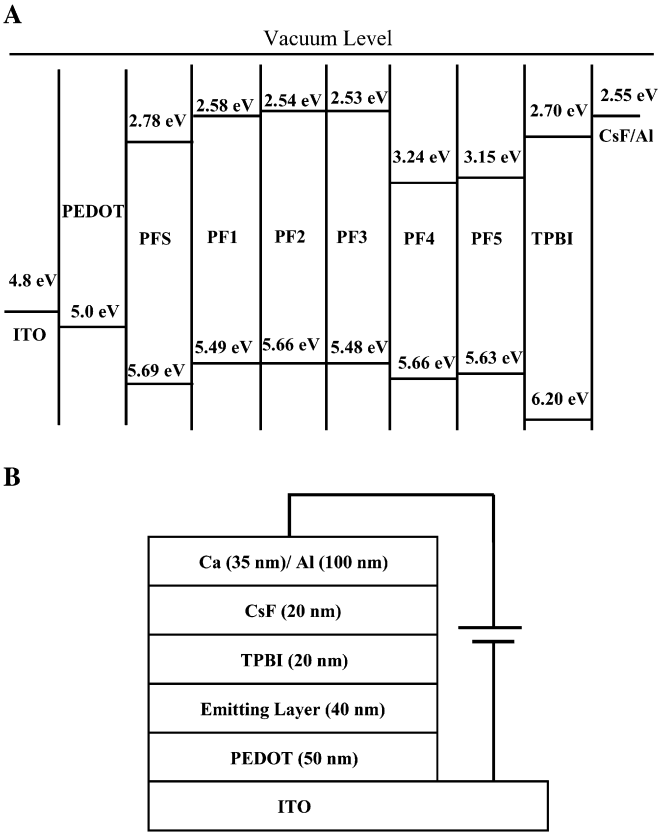

Fig. 4. Energy level diagram and device structure of the studied polyfluorene polymers.

electroluminescent performance of **PFS** and sulfide-containing polyfluorene (**PF1**, **PF3** and **PF4**) in device B. The maximum luminance of **PF1** was increased from 990 to 2991 cd/m^2, and the maximum efficiency was also improved from 0.15 (330 mA/cm^2) to 1.36 cd/A (75 mA/cm^2). In the **PF4**-based systems, the maximum brightness also increased from 1743

Table 4
Device performance of polyfluorene based on polymers **PFS**, **PF1–PF5**

Polymer	Device structure	L_{max} (cd/m^2) at voltage (V)	Yield$_{max}$ (cd/A)	EL λ_{max} (nm)	CIE coordinate 1931 (X,Y)
PFS	A	450 at 10 V	0.19	444	0.18,0.20
PFS	B	804 at 10 V	0.27	448	0.20,0.20
PFS	C	521 at 11 V	0.72	444	0.18,0.20
PF1	A	990 at 10 V	0.15	464	0.21,0.25
PF1	B	2991 at 8 V	1.36	468	0.21,0.23
PF1	C	1832 at 10 V	1.49	464	0.21,0.23
PF2	A	1002 at 10 V	0.23	472	0.24,0.27
PF3	A	700 at 11 V	0.12	464	0.20,0.26
PF3	B	800 at 10 V	0.34	464	0.22,0.26
PF3	C	686 at 10 V	1.65	464	0.20,0.26
PF4	A	1743 at 11 V	0.60	540	0.41,0.57
PF4	B	2640 at 10 V	1.23	540	0.39,0.54
PF4	C	2868 at 10 V	2.47	540	0.40,0.54
PF5	A	1962 at 10 V	0.85	544	0.43,0.55

Device A: ITO/PEDOT:PSS/polymer (40 nm)/Ca (35 nm)/Al (100 nm), device B: ITO/PEDOT:PSS/polymer (40 nm)/CsF (2 nm)/Al (100 nm), device C: ITO/PEDOT:PSS/polymer (40 nm)/TPBI (2 nm)/CsF (2 nm)/Al (100 nm).

to 2868 cd/m^2 and the maximum efficiency could be increased from 0.60 (220 mA/cm^2) to 1.23 cd/A (57 mA/cm^2).

In device C, a thin TPBI layer that acts as an electron transport and hole-blocking layer, was deposited between emitting layer and CsF by a thermal-evaporation method. The detailed device structure is ITO/PEDOT:PSS/polymer (40 nm)/TPBI (2 nm)/CsF (2 nm)/Al (100 nm). Fig. 5, in parts A, B and C, shows the current–voltage, luminescence–voltage and current–efficiency characteristics, respectively, of **PF1** based on the different devices. Obviously, the one with the electron transporting TPBI layer shows the highest efficiency of 1.49 cd/A (20 mA/cm^2). Similar results were also seen in the **PF3** and **PF4**-based devices, for which the maximum efficiency was improved from 0.12 (636 mA/cm^2) to 1.65 cd/A (21 mA/cm^2) and from 0.60 (220 mA/cm^2) to 2.47 cd/A (11 mA/cm^2), respectively (Table 4). Fig. 6 shows the EL spectra of **PF1** which emitted sky-blue light under different voltages in device A. The EL spectrum is nearly identical with respect to position and curve shape, indicating that both PL and EL originate from the same radiative decay process of the single exciton. However, under device operation, the undesirable low energy emission band (between 500 and 600 nm) does not appear in the **PF1** device. Similar phenomenon was also observed in the case of **PF3**. These sulfide-containing blue-light polyfluorene polymers exhibit a voltage-independent and stable EL spectrum. This finding was also in consistence with the annealing test mentioned above—that sulfur atom suppresses the keto formation and polymer chain aggregation.

3.7. Formation and characterization of the nanocomposites

The sulfur atom in monomer **M3** can serve as the ligand for **CdSe/ZnS** quantum dots (QDs) in the final nanocomposites obtained via ligand exchange procedure. These nanocomposites are also soluble in common organic solvents, such as toluene, THF, and chloroform. The FT-IR spectroscopy technique was applied to verify the chemical structure of the organic/inorganic hybrid material. Fig. 7(A) shows the FT-IR spectra of **PF1**, **PF1** grafted with **CdSe/ZnS** nanocomposite and **CdSe/ZnS** quantum dots. The FT-IR spectrum of **CdSe/ZnS** quantum dots around 3000 cm^{-1} is attributed to the C–H stretching of the out shell alkyl surfactant, trioctylphosphine oxide (TOPO). It is obvious that two new bands were formed around 1000–1100 cm^{-1} after ligand exchange process, which are attributed to the force formation between sulfur and **CdSe/ZnS**. Similar observations were also found for other nanocomposites. This finding is consistent with the literature reports [24,25]. The TGA measurements were made up to 750 °C, and the residue was considered to be char (from polymers) and **CdSe/ZnS**. By subtracting the char content, the **CdSe/ZnS** content in the polymer was determined to be 10.1 and 6.6 wt% for **PF1–CdSe** and **PF4–CdSe**. By grafting CdSe with polyfluorenes, a hard block of phase-separated graft copolymer would form that effectively suppresses the chain mobility and packing ability, and thus slightly improves the thermal stability. The decomposition temperatures of

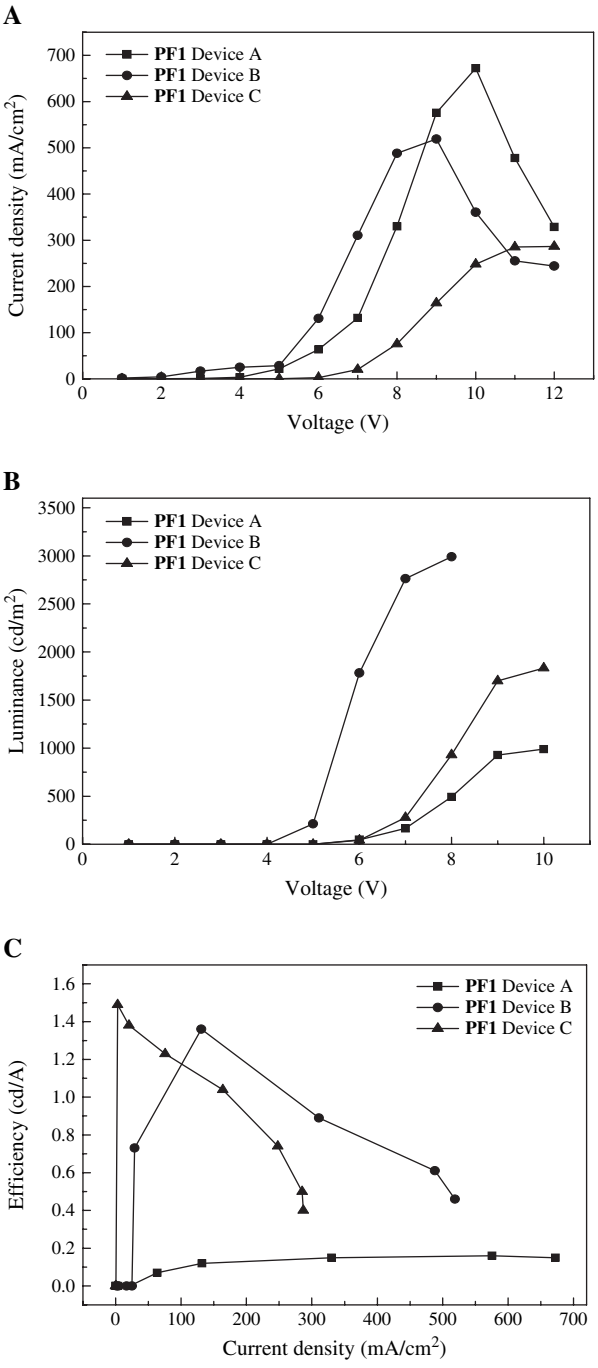

Fig. 5. (A) Voltage–current density, (B) Luminance–voltage, and (C) efficiency–current density characteristics of the fluorene-based polymers **PFS** and **PF1–PF5** in different device structures. Device A – ITO/PEDOT:PSS/polymer (40 nm)/Ca (35 nm)/Al (100 nm), device B – ITO/PEDOT:PSS/polymer (40 nm)/CsF (2 nm)/Al (100 nm), device C – ITO/PEDOT:PSS/polymer (40 nm)/TPBI (2 nm)/CsF (2 nm)/Al (100 nm).

polyfluorene derivatives and their nanocomposites with QDs are in the range from 344 to 373 °C, as shown in Fig. 7(B). All the QDs-containing polymers exhibit better thermal stability over the original, pristine polymers. The higher T_d values obviously suggest that the incorporation of inorganic QDs into polyfluorenes could effectively enhance the thermal stability. Fig. 8 shows the normalized photoluminescence (PL)

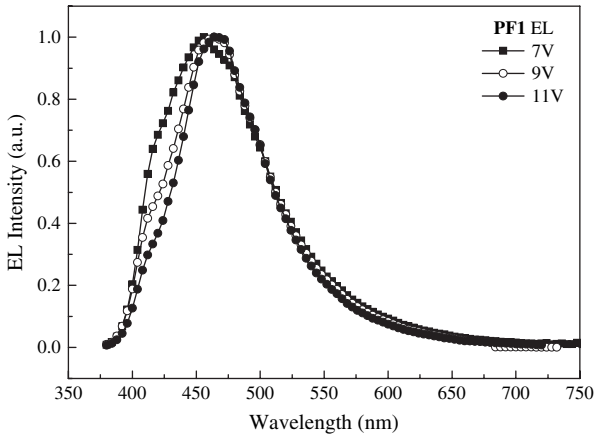

Fig. 6. EL spectra of polymer **PF1** at different voltages in device A.

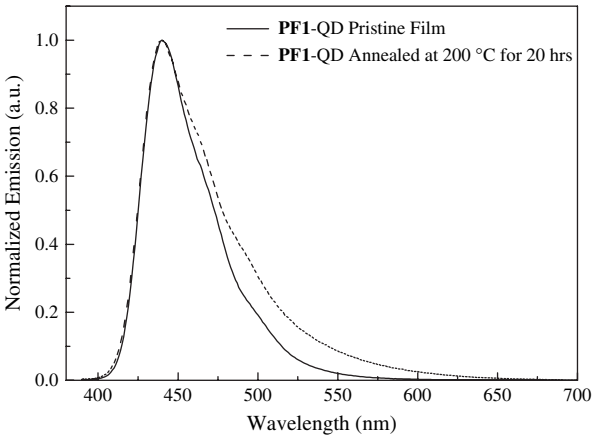

Fig. 8. Normalized PL spectra of **PF1−CdSe/ZnS** nanocomposite in solid state before and after annealing at 200 °C for 20 h under air.

spectra of the **PF1−CdSe** nanocomposite films before and after thermally annealed at 200 °C for 20 h. First of all, the emission curve of **PF1−CdSe** nanocomposite is similar to pristine polymer **PF1** without CdSe moiety, with a longer wavelength at 440 nm. This phenomenon also suggests that inserting CdSe component does not affect the optical properties of polymer backbone. It is obvious that the PL spectrum of **PF1−CdSe** nanocomposite shows a small shoulder under heating conditions, this is similar to the case of homopolymer **PFS**. The unchanged emission λ_{max} in the annealing test deeply indicates that sulfide-containing polyfluorene effectively restrains the ketone formation and aggregation of polymer chains under thermal annealing.

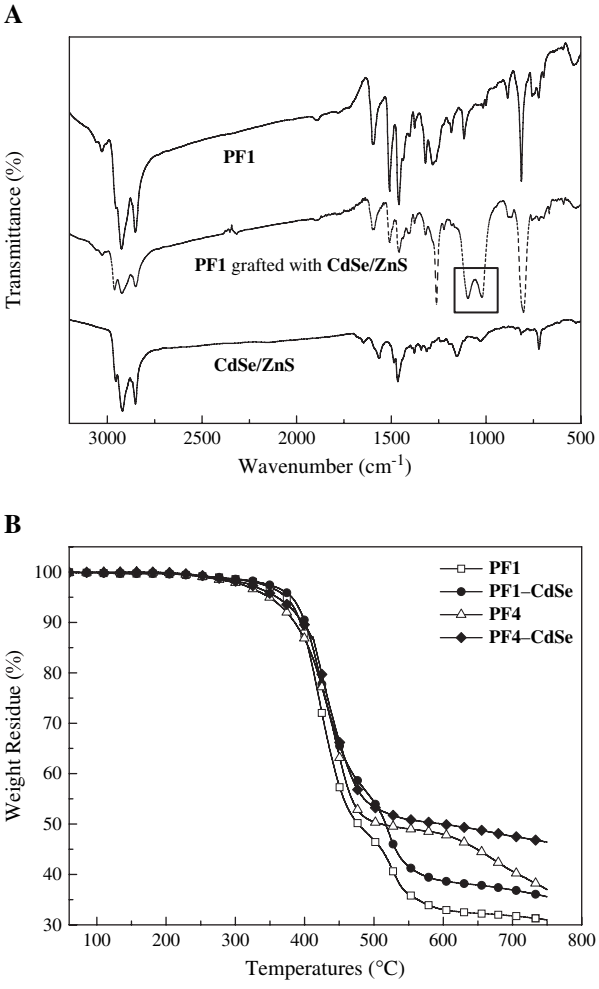

Fig. 7. (A) FT-IR spectra of **PF1**, **PF1−CdSe/ZnS** nanocomposite and **CdSe/ZnS**. (B) TGA thermograms of polymer **PF1**, **PF4** and nanocomposites (**PF1−CdSe**, **PF4−CdSe**) under N_2 atmosphere.

To identify the EL properties of the nanocomposite, both the pristine polymers and QDs-containing polymers were used as the emitting layers in a double-layer light-emitting device of ITO/PEDOT:PSS/polymer/Ca/Al configuration. Fig. 9 shows the current−voltage, luminescence and yield−voltage characteristics of the devices based on **PF1−CdSe** and pristine **PF1**. It is seen that the current densities of **PF1−CdSe** devices are much lower than that of pristine **PF1**. The luminance was increased from 990 to 1536 cd/m^2, and the efficiency was also be improved from 0.15 (330 mA/cm^2) to 0.78 cd/A (65 mA/cm^2). The similar results were also seen in the **PF4**-based devices, for which the maximum brightness was also increased from 1743 to 2847 cd/m^2 and the maximum efficiency was increased from 0.60 (220 mA/cm^2) to 1.74 cd/A (61 mA/cm^2). Polyfluorene is a well-known hole-dominating material, and the mobility of holes and electrons is not very much balanced. To consider direct charge injection, holes were blocked at CdSe owing to the relatively low-lying HOMO energy level. This can also be verified from the decreased current density under the same driving voltage. The blocked holes were accumulated and recombined with electrons to form excitons in the emitting layer. This suggests that incorporation of CdSe restrains the charge flow substantially throughout the device and increases the probability of excitons' formation. Balanced hole and electron transports are thus achieved; the performance and efficiency of the device are also improved.

3.8. Hole-only and electron-only devices

In general devices, holes are injected from the PEDOT:PSS contact into the polyfluorene emitting layer and transported

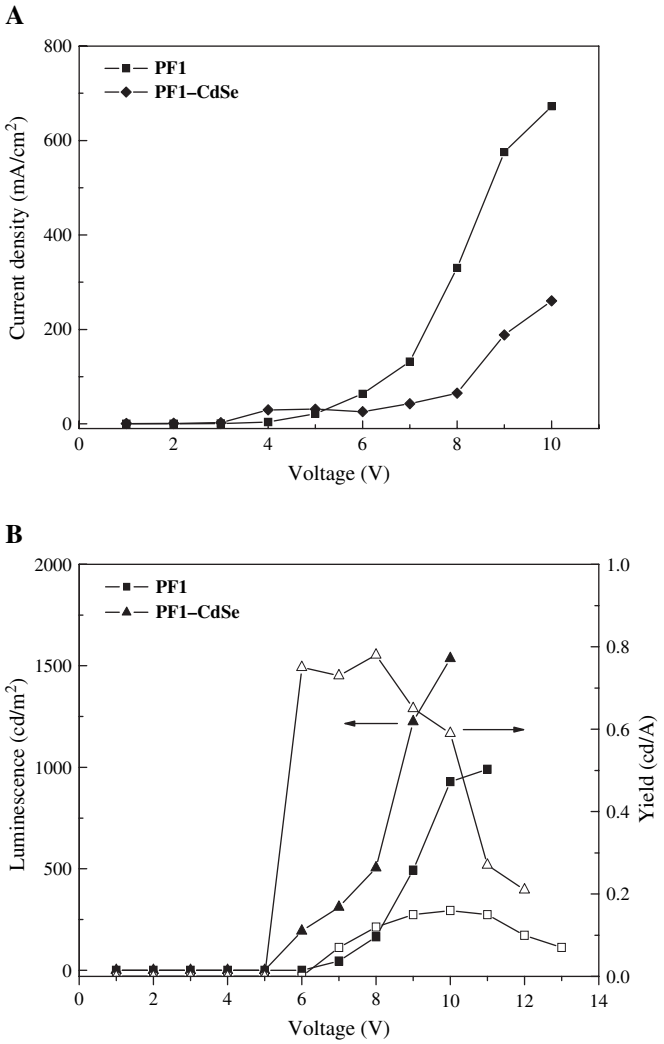

Fig. 9. (A) Voltage–current density, (B) luminescence–voltage efficiency characteristics of the **PF1** and nanocomposite LED devices.

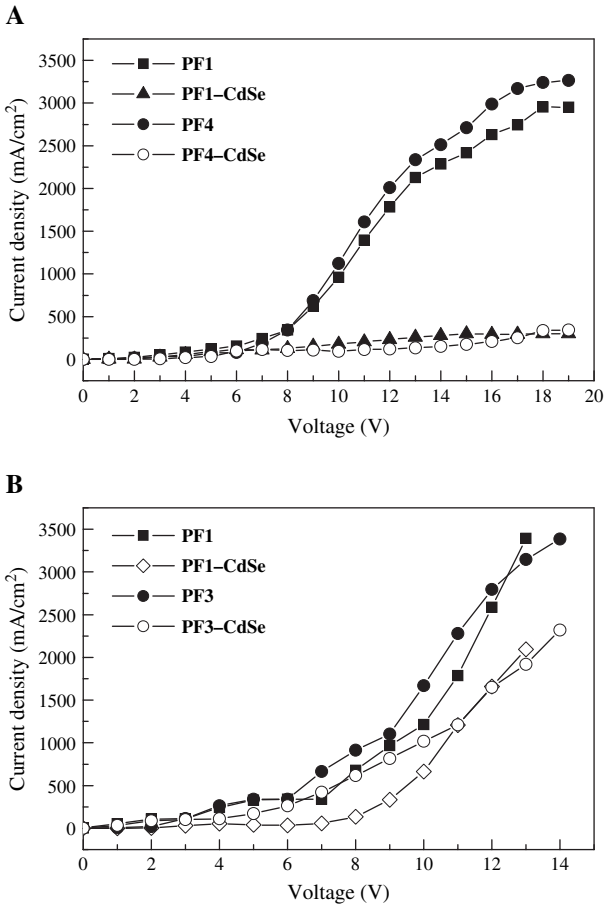

Fig. 10. $J-V$ characteristic of (A) ITO/PEDOT/polymer or nanocomposite/Au hole-only device, (B) ITO/Al/polymer or nanocomposite/Ca/Al electron-only device with a thickness around $L = 0.040-0.045$ μm.

toward the cathode. Hole-only and electron-only devices were prepared to characterize the current transport properties of the nanocomposites [38,39]. In Fig. 10, the $J-V$ characteristics of several ITO/PEDOT/polymers/Au "hole-only" and ITO/Al/polymers/Ca/Al "electron-only" devices were presented; the current was reduced substantially in both cases. It also indicates that QDs decrease the charge mobility and result in higher efficiency for these nanocomposite devices. The hole-blocking ability of QDs is stronger than the electron trapping ability. For these nano-sized QDs-containing devices, some of the injected holes were blocked by QDs in the light-emitting layer, resulting in better recombination of carriers in the polymer layer than that without QDs.

4. Conclusions

In this paper, we have established synthetic approaches to four sulfide-containing polyfluorene derivatives (**PFS**, **PF1–PF3**). These polymers show higher T_g and T_d values than their corresponding alkyl-substituted polyfluorenes. FT-IR and PL spectral studies of thermal annealing tests demonstrate that the incorporation of the sulfur atom into the polyfluorene could effectively suppress the 'keto-defect' which is commonly observed in polyfluorenes. This means that sulfur-containing polymers are less susceptible to oxidation. The **CdSe/ZnS** was grafted to the sulfur atoms by the ligand exchange reaction. FT-IR spectra display two new peaks around 1000–1100 cm^{-1}, indicating new force formation between sulfur from polyfluorene and CdSe. As **CdSe/ZnS** was incorporated onto polymers via chemical bonding, the device performance was significantly increased as compared to their parent polymers alone. The electrical characteristics of the diodes reveal that QDs could effectively increase the luminance and reduce the current density of devices. Hole-only and electron-only devices fabricated from these nanocomposites demonstrate that **CdSe/ZnS** QDs exactly block the hole and trap the electron in the light-emitting layer, respectively. Consequently, the electroluminescent efficiency of the light-emitting materials was effectively improved. The present chemical bonding process of nano-sized materials and conjugated polymers may offer a general strategy for fabricating high-performance light-emitting materials.

Acknowledgements

The authors are grateful to the National Science Council (NSC95-2120-M-009-001) and Ministry of Education (MOE ATU Program) of the Republic of China for the financial support of this work.

References

[1] Burroughes JH, Bradley DDC, Brown AR, Marks RN, Mackay K, Friend RH, et al. Nature 1990;347:539.
[2] Bradley DDC, Grell M, Long X, Mellor H, Grue A, Inbasekaran H, et al. Proc SPIE Int Soc Opt Eng 1997;3145:254.
[3] (a) Kreyenschmidt M, Klaerner G, Fuhrer T, Ashenhurst J, Karg S, Chen WD, et al. Macromolecules 1998;31:1099;
(b) Lee JI, Klärner G, Miller RD. Chem Mater 1999;11:1083;
(c) Klärner G, Lee JI, Lee VY, Chan E, Chen JP, Nelson A, et al. Chem Mater 1999;11:1800;
(d) Klärner G, Lee JI, Davey MH, Miller RD. Adv Mater 1999;11:115.
[4] (a) Setayesh S, Grimsdale AC, Weil T, Enkelmann V, Müllen K, Meghdadi F, et al. J Am Chem Soc 2001;123:946;
(b) Jacob J, Zhang J, Grimsdale AC, Müllen K, Gaal M, List EJW. Macromolecules 2003;36:8240.
[5] Marsitzky D, Murray J, Scott JC, Carter KR. Chem Mater 2001;13:4285.
[6] Lim E, Jung BJ, Shim HK. Macromolecules 2003;36:4288.
[7] Gaal M, List EJW, Scherf U. Macromolecules 2003;36:4236.
[8] Cho HJ, Jung BJ, Cho NS, Lee J, Shim HK. Macromolecules 2003;36:6704.
[9] Bliznyuk VN, Carter SA, Scott JC, Klärner G, Miller RD, Miller DC. Macromolecules 1999;32:361.
[10] Yu WL, Pei J, Cao Y, Huang W, Heeger AJ. Chem Commun 1999;1837.
[11] Pei J, Yu WL, Huang W, Heeger AJ. Chem Commun 2000;1631.
[12] Kulkarni AP, Jenekhe SA. Macromolecules 2003;36:5285.
[13] (a) Chou CH, Shu CF. Macromolecules 2002;35:9673;
(b) Shu CF, Dodda R, Wu FI, Liu MS, Jen AKY. Macromolecules 2003;36:6698.
[14] (a) Marsitzky D, Vestberg R, Blainey P, Tang BT, Hawker CJ, Carter KR. J Am Chem Soc 2001;123:6965;
(b) Tang HZ, Fujiki M, Zhang ZB, Torimitsub K, Motonaga M. Chem Commun 2001;2426.
[15] Inaoka S, Advincula R. Macromolecules 2002;35:2426.
[16] Yu WL, Pei J, Huang W, Heeger AJ. Adv Mater 2000;12:828.
[17] Zeng G, Yu WL, Chua SJ, Huang W. Macromolecules 2002;35:6907.
[18] Vak D, Chun C, Lee CL, Kim JJ, Kim DY. J Mater Chem 2004;14:1342.
[19] Tamaki R, Tanaka Y, Asuncion MZ, Choi J, Laine RM. J Am Chem Soc 2001;123:12416.
[20] (a) Xiao S, Nguyen M, Gong X, Cao Y, Wu H, Moses D, et al. Adv Funct Mater 2003;13:25;
(b) Lin WJ, Chen WC, Wu WC, Niu YH, Jen AKY. Macromolecules 2004;37:2335.
[21] (a) Carter SA, Scott JC, Brock PJ. Appl Phys Lett 1997;71:1145;
(b) Kim YK, Lee KY, Kwon OK, Shin DM, Sohn BC, Choi JH. Synth Met 2000;111–112:207.
[22] Lee K, Sariciftci NS, Heeger AJ. Synth Met 1995;69:445.
[23] (a) Lim YT, Lee TW, Lee HC, Park OO. Synth Met 2002;128:133;
(b) Park JH, Lim YT, Park OO, Kim JK, Yu JW, Kim YC. Chem Mater 2004;16:688.
[24] Chou CH, Wang HS, Wei KH, Huang JY. Adv Funct Mater 2006;16:909.
[25] Chen KB, Chen MH, Yang SH, Hsieh CH, Hsu CS, Chen CC, et al. J Polym Sci Part A Polym Chem 2006;44:5378.
[26] Woo EP, Inbasekaran M, Shiang W, Roof GR. International Patent WO 97/05184; 1997.
[27] Beulen MWJ, Kastenberg MI, Van Veggel FCJM, Reinhoudt DN. Langmuir 1998;14:7463.
[28] Pilgram K, Zupan M, Skiles R. J Heterocycl Chem 1970;7:629.
[29] Klärner G, Miller RD. Macromolecules 1998;31:2007.
[30] Miteva T, Meisel A, Knoll W, Nothofer HG, Scherf U, Müller DC, et al. Adv Mater 2001;13:565.
[31] Miyaura N, Suzuki A. Chem Rev 1995;95:2457.
[32] Ding J, Day M, Robertson G, Roovers J. Macromolecules 2002;35:3474.
[33] Zhou X, He J, Liao LS, Lu M, Ding XM, Hou XY, et al. Adv Mater 2000;12:265.
[34] Leeuw DM, Simenon MMJ, Brown AR, Einerhand REF. Synth Met 1997;87:53.
[35] Fang Q, Yamamoto T. Macromolecules 2004;37:5894.
[36] Piromreun P, Oh H, Shen Y, Malliaras GG, Scott JC, Brock PJ. Appl Phys Lett 2000;77:2403.
[37] Locklin J, Patton D, Deng S, Baba A, Millan M, Advincula RC. Chem Mater 2004;16:5187.
[38] Manabe K, Hu W, Matsumura M, Naito H. J Appl Phys 2003;94:2024.
[39] Chirbase D, Chiguvare Z, Knipper M, Parisi J, Dyakonov V, Hummelen JC. J Appl Phys 2003;93:3376.